

秦燕, 徐衍明, 侯可军, 等. 铁同位素分析测试技术研究进展[J]. 岩矿测试, 2020, 39(2): 151 - 161.

QIN Yan, XU Yan-ming, HOU Ke-jun, et al. Progress of Analytical Techniques for Stable Iron Isotopes[J]. Rock and Mineral Analysis, 2020, 39(2): 151 - 161.

[DOI: 10.15898/j.cnki.11-2131/td.201908120120]

铁同位素分析测试技术研究进展

秦燕¹, 徐衍明², 侯可军^{1*}, 李延河¹, 陈蕾¹

(1. 自然资源部成矿作用与资源评价重点实验室, 中国地质科学院矿产资源研究所, 北京 100037;

2. 青岛地质工程勘察院(青岛地质勘查开发局), 山东 青岛 266071)

摘要: 铁是地球上丰度最高的变价元素, 在自然界大量分布于各类矿物、岩石、流体和生物体中, 并广泛参与成岩作用、成矿作用、热液活动和生命活动过程。铁同位素组成对地球化学、天体化学和生物化学方面提供重要的信息, 是同位素地球化学研究领域的热点。铁同位素的精确测量是开展相关研究的重要基础。本文评述了铁同位素测试技术的研究进展, 主要包括: ①溶液法测试铁同位素样品纯化过程中阴离子树脂的改进; ②质谱分析从传统的热电离质谱法发展为多接收电感耦合等离子体质谱法; ③激光微区原位测试技术的研发等。在此基础上, 对测试过程中会导致产生铁同位素分馏的步骤和校正方法进行了总结, 并对各种测试方法的优缺点进行了评述。本文认为: 溶液法分析流程长且复杂, 但分析精度高(0.03‰, 2SD)、方法稳定; 微区原位分析方法从纳秒激光剥蚀发展为飞秒激光剥蚀, 脉冲持续时间更短、脉冲峰值强度更高(可达 10^{12} W), 聚焦强度超过 10^{20} W/cm², 使其具有分析速度快、空间分辨率高的优势。微区原位法可以从微观角度去讨论铁同位素变化的地球化学过程, 但基体效应的存在限制了微区原位铁同位素的广泛应用。因此, 缩短溶液法分析流程, 开发系列基体匹配的标准样品, 是铁同位素分析方法研发的方向。

关键词: 铁同位素; 化学提纯; 溶液法; 质谱; 激光剥蚀; 基体效应

要点:

- (1) 总结了铁同位素测试技术的研究进展。
- (2) 归纳了测试过程产生同位素分馏的机制和校正方法。
- (3) 对比了溶液法和微区原位铁同位素测试方法的优缺点。

中图分类号: O628 **文献标识码:** A

铁的原子序数为 26, 属于过渡族金属元素, 是地壳中含量居第四的金属元素。铁具有亲氧和亲硫的性质, 除了形成氧化物和含氧酸盐的矿物质之外, 还可以形成众多的硫化物和硫酸盐的矿物^[1-2]。由于铁是变价元素(0 价、+2 价、+3 价), 可以广泛地与其他金属离子发生置换, 地球上含铁的矿物高达 300 多种^[3]。铁也是太阳系最重要的金属元素和类地行星的主要构成元素^[4]。此外, 铁是生物体不可或缺的元素, 地球上各种生物化学作用均有铁的参与^[3,5-7]。铁有 4 个稳定同位素, 其丰度分别为:

⁵⁴Fe(5.82%)、⁵⁶Fe(91.66%)、⁵⁷Fe(2.19%)、⁵⁸Fe(0.33%)。在自然界各物质间铁同位素具有一定的差异^[1], 由于铁的广泛分布, 铁同位素组成变化对于研究成矿作用、岩浆过程、天体化学、古环境演化和生物化学等方面显示巨大的潜力。

近年来, 铁同位素地球化学在地球科学领域的研究主要集中在以下四个方面: ①地球主要储库的铁同位素组成^[8-15]。②高温地质过程铁同位素的分馏行为, 如地幔部分熔融与交代过程、地壳部分熔融、岩浆分异等过程^[16-21]。③低温过程如生物作用、风化作

收稿日期: 2019-08-12; 修回日期: 2019-09-17; 接受日期: 2019-10-21

基金项目: 中央级公益性科研院所基本科研业务费专项(JYYWF20180104)

作者简介: 秦燕, 博士, 副研究员, 主要研究方向为同位素地球化学。E-mail: happyqinyan@sina.com。

通信作者: 侯可军, 博士, 副研究员, 主要研究方向为同位素地球化学。E-mail: kejunhou@126.com。

用和早期成岩作用中铁同位素的分馏特征^[22-24]。

④示踪生物活动和指示古海洋循环^[25-26]。此外,铁同位素在宇宙化学和行星科学也得到了广泛的应用^[27-28]。由于自然界铁同位素分馏较小^[8],铁同位素的精确测定是开展各项应用的重要前提。

最早的铁同位素分析采用热电离质谱法(TIMS),在进行铁同位素测定时无法使用内标法进行仪器的质量分馏校正,导致测试误差较大。又因为与硫、氧等传统稳定同位素相比,铁同位素组成在自然界变化较小,传统的TIMS测试方法难以满足地质工作的需要。直到Belshaw等^[29]于2000年建立了铁同位素的多接收电感耦合等离子体质谱(MC-ICP-MS)测定方法,使得铁、铜、锌等非传统稳定同位素的测试技术取得了突破性进展,高精度的铁同位素分析技术成为现实。为获得高精度的铁同位素数据,无论是溶液法还是激光原位法,样品纯度、测试过程中的质量歧视校正和干扰扣除都至关重要。本文阐述了铁同位素测试常用的化学分离纯化方法和主要仪器分析技术研究进展,评述了各种方法的优缺点及适用领域,旨在促进铁同位素在地球科学领域的技术支撑作用。

1 铁同位素表示方法及标准样品

铁同位素组成的表示方法为:

$$\delta^x\text{Fe} = \left[\frac{({}^{56}\text{Fe}/{}^{54}\text{Fe})_{\text{样品}}}{({}^{56}\text{Fe}/{}^{54}\text{Fe})_{\text{标准}}} - 1 \right] \times 1000$$

$$\varepsilon^x\text{Fe} = \left[\frac{({}^{56}\text{Fe}/{}^{54}\text{Fe})_{\text{样品}}}{({}^{56}\text{Fe}/{}^{54}\text{Fe})_{\text{标准}}} - 1 \right] \times 10000 \quad (x=56,57)$$

大部分文献中,铁同位素数据采用 $\delta^{56}\text{Fe}$ 进行讨论,也有部分学者用 $\delta^{57}\text{Fe}$ 、 $\varepsilon^{56}\text{Fe}$ 、 $\varepsilon^{57}\text{Fe}$ 。本文出现的精度数据均以 $\delta^{56}\text{Fe}(2\text{SD})$ 为标准进行讨论。

早期使用的铁同位素标准物质为15块地球火成岩和5块高钛月球玄武岩的平均值(MIR),后续研究表明火成岩中存在显著的铁同位素分馏而被弃用^[1,9]。现今国内外常用的铁同位素标准物质是由欧洲标准局参考物质及测量研究所推出的IRMM-014 Fe(铁丝,纯度99.99%)^[29]。基于这两种标准的数据转换关系为: $\delta^{56}\text{Fe}_{\text{IRMM-014}} = \delta^{56}\text{Fe}_{\text{MIR}} + 0.09\text{‰}$ 。除此之外,国内外实验室还经常使用包括美国地质调查局在内的岩石粉末标准样品,如BCR-1、BCR-2、AGV-2等作为实验室标准,进行重现性和准确度对比测试。由于铁同位素国际标准物质十分匮乏,开展标准物质的研发工作十分必要,我国进行铁同位素标样研制工作的主要有唐索寒等^[30]。

2 铁同位素分析方法

由于铁同位素在自然界中的分馏较小,为了识别不同样品的铁同位素差异,对其测试方法的精度需要极高的要求。最早建立能有效识别各种地球化学过程铁同位素比值变化的方法是将样品全部溶解、纯化,采用溶液进行质谱测定,这种方法得到的是整个样品同位素组成的平均值。近年来发展起来的激光原位分析法则通过激光将样品剥蚀出细小的气溶胶,电离后进入质谱仪进行测定的方法,可以获得矿物微区尺度同位素变化的特征。

2.1 溶液进样法

由于铁是主要的造岩元素,所以将其从原岩中提取出来比较简单。本实验室操作步骤一般为:根据样品的性质选择合适的酸(盐酸、硝酸、氢氟酸、醋酸等)和过氧化氢将样品全部消解,且保证Fe为+3价。加入盐酸重复2次蒸干后转入盐酸介质,等待过柱纯化样品^[29,31-32]。溶液进样分析法中样品纯化和质谱测定是关键的两个步骤。

2.1.1 样品纯化

由于大多数天然样品具有复杂的化学成分,应用质谱进行铁同位素测试时会存在一系列的谱峰干扰信号(表1)或导致测试过程中仪器质量歧视的变化,即所谓的基质效应^[33-35]。这些干扰大致可以分为两类:一类是多原子离子干扰,如氩等离子体源在高温下产生的 $[{}^{40}\text{Ar}^{14}\text{N}]^+$ 、 $[{}^{40}\text{Ar}^{16}\text{O}]^+$ 等,以及 $[{}^{40}\text{Ca}^{14}\text{N}]^+$ 、 $[{}^{27}\text{Al}^{27}\text{Al}]^+$ 等离子团,这类干扰通常可以通过高分辨率模式将其与待测同位素区分开来;另一类是同质异位素干扰,它们的核子质量非常接近,如 ${}^{54}\text{Cr}^+$ 、 ${}^{58}\text{Ni}^+$ 等,一般的磁式质谱仪分辨率无法将其分开,必须使用化学提纯法加以去除。因此,在进行同位素质谱分析之前,进行高精度的样品纯化十分必要。

表1 某些潜在的铁同位素谱峰干扰信号^[35]

Table 1 Some potential isobaric interferences on Fe isotope signals^[35]

质量数	待测核素	同质异位素	多原子离子
54	${}^{54}\text{Fe}^+$	${}^{54}\text{Cr}^+$	$[{}^{40}\text{Ar}^{14}\text{N}]^+$, $[{}^{27}\text{Al}^{27}\text{Al}]^+$, $[{}^{40}\text{Ca}^{14}\text{N}]^+$, $[{}^{42}\text{Ca}^{12}\text{C}]^+$
56	${}^{56}\text{Fe}^+$	-	$[{}^{40}\text{Ar}^{16}\text{O}]^+$, $[{}^{42}\text{Ca}^{14}\text{N}]^+$, $[{}^{28}\text{Si}^{28}\text{Si}]^+$
57	${}^{57}\text{Fe}^+$	-	$[{}^{40}\text{Ar}^{17}\text{O}]^+$, $[{}^{40}\text{Ar}^{16}\text{O}^1\text{H}]^+$
58	${}^{58}\text{Fe}^+$	${}^{58}\text{Ni}^+$	$[{}^{40}\text{Ar}^{18}\text{O}]^+$

Kraus 等(1953)^[36]首次使用不同浓度的盐酸通过 Dowex - 1 强碱性阴离子交换树脂对铜、铁元素进行洗脱分离,文中提出高浓度(约 10mol/L)的盐酸有利于将 Fe^{3+} 与 Cu^{2+} 等其他离子分开,但文章中并没有对洗脱效率进行定量说明。随后的几十年中,各种类型阴离子交换柱开始应用到不同地质样品中的铁分离提纯工作中,主要有 Dowex1、AG1 和 Amberlite IRA - 400 这三种^[37]。阴离子树脂分离铁离子的工作原理是:阴离子交换树脂具有活性基团,在高浓度酸中 Fe^{3+} 与 Cl^- 结合,被阴离子树脂活性基团所吸附,而其他一些基质元素(Cr、Ni 等)极易从树脂上洗脱。根据这些络阴离子与交换树脂亲和力的差异,选择适宜的酸和酸度,可将 Fe 元素与其他元素分离^[38-40]。

1980 年,Strelow^[38]通过洗脱曲线和定量分析结果提出了 8mol/L 盐酸在 AG1 - X4 阴离子交换柱上可以对溶液中 Cu^{2+} 、 Mn^{2+} 、 Ni^+ 、 Al^{3+} 、 Mg^{2+} 等干扰离子进行有效洗脱,但对 Ti、Zr、Hf、Cr 元素的洗脱效果没有进行检测。van der Walt 等(1985)^[41]指出盐酸介质中 Fe、Cu、Zn 三种元素在 AG MP - 1 强碱性阴离子大孔径树脂中承载量更大。Marechal 等(1999)^[42]建立了采用强碱性阴离子交换树脂 AG MP - 1 在不同浓度的盐酸条件下同时分离纯化 Fe、Cu、Zn 的方法。随后,学者们纯化样品中铁同位素主要集中到 AG1 - X4、X8 或 AG MP - 1 两大类离子交换树脂^[39,42-44]。AG1 - X4、X8 和 AG MP - 1 都是阴离子交换树脂,前者更精细,后两者是大孔径树脂,样品承载量更大。前人对这两大类离子交换树脂对金属离子纯化效果,开展了大量研究工作^[45-48]。在用酸量上,AG1 - X4 微型离子交换柱的盐酸用量较少,可以很好地将 Fe 与其他元素分离,同时缩短了分离流程,减少了分离和蒸干样品的时间^[45,49]。AG MP - 1 分离铁会使淋洗曲线变宽,能避免铁与其他元素有交叉,减少干扰元素和基体效应^[40,50-51]。

本实验室采用 AG MP - 1 大孔隙阴离子树脂为交换体,以 2mol/L 盐酸、7mol/L 盐酸、0.5mol/L 硝酸为介质,可同时进行 Fe、Cu、Zn 元素的高纯度分离(图 1),Fe 元素的回收率可达 99% ~ 102%,Fe 的流程空白仅有 0.026 μg ,远小于样品量的 0.1%,不会对测试结果产生影响^[33]。

2.1.2 质谱测定

铁同位素质谱测试主要有两种方法:传统的热电离质谱法(TIMS)和多接收电感耦合等离子体

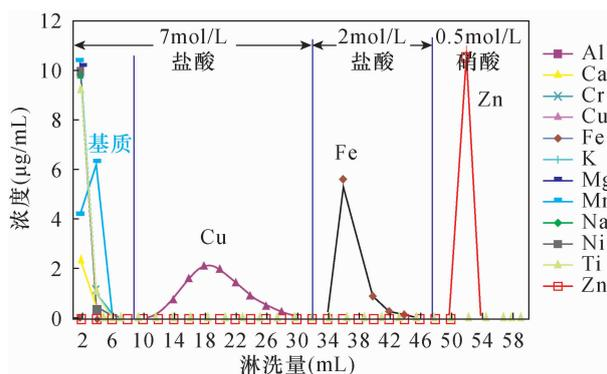


图 1 Fe 与基质的化学分离淋洗曲线^[33]

Fig. 1 Elution curve for Fe element separation

质谱法(MC - ICP - MS)。

(1) 热电离质谱法

铁同位素测试最早是由 Taylor (1992) 采用 TIMS 法完成的。由于 TIMS 进行铁同位素测定时无法用内标法进行仪器的质量分馏校正,导致测试误差较大^[52]。直到 20 世纪末,双稀释剂 TIMS 铁同位素方法的建立,使得铁同位素测试精度得到很大提高, $\delta^{56}\text{Fe}$ 的测试精度达 0.6‰(2SD),虽然仍然有许多自然样品的铁同位素组成无法得到精确测定,但对开展铁同位素系统测定的研究发挥了重要的推进作用^[29,53]。此外,TIMS 存在其他的技术缺陷,如:电离源的温度只有 2000℃ 左右,铁的离子化效率较低,同时测试耗时,操作过程也比较复杂^[51,53]。因此,使用 TIMS 测定的铁同位素比值仍然无法有效识别很多地质过程的同位素变化。

(2) 多接收电感耦合等离子体质谱法

多接收电感耦合等离子体质谱是 20 世纪 90 年代中后期研发的一种质谱仪。其显著特点是具有双聚焦、中高分辨功能和配置有多个法拉第接收杯(Faraday cup)和离子计数器。Belshaw 等^[29]和 Zhu 等^[54]率先建立了铁同位素的 MC - ICP - MS 测定方法。MC - ICP - MS 的出现使得高精度铁同位素测定成为现实。与双稀释剂 TIMS 方法相比,MC - ICP - MS 的 Ar 离子源可以产生很高的温度,离子化效率较高,分析速度快^[29]。目前,适用铁同位素高精度分析的 MC - ICP - MS 仪器类型主要有 Nu Plasma 高分辨(HR)型、1700 型以及 ThermoFinnigan 公司的 Neptune、Neptune Plus 型 MC - ICP - MS。

如前所述, $[\text{}^{40}\text{Ar}^{14}\text{N}]^+$ 、 $[\text{}^{40}\text{Ar}^{16}\text{O}]^+$ 、 $[\text{}^{40}\text{Ar}^{17}\text{O}]^+$ 这些多原子离子干扰无法通过化学分离去除,它们与目标核素 $^{54}\text{Fe}^+$ 、 $^{56}\text{Fe}^+$ 、 $^{57}\text{Fe}^+$ 分开需要至少 2500 的分辨率。早期各实验室尝试盐酸介

质进样+膜去溶技术、冷等离子体和碰撞池技术来抑制含氩基团的产生^[31,38-39,55]。随着仪器技术的发展,Neptune型或Nu型多接收电感耦合等离子体质谱通过调节离子入射狭缝宽度,中分辨模式下能够达到大约8000的分辨率,而高分辨率模式下分辨率可达10000~12000,能够将干扰元素离子团和目标同位素分离^[56-57]。图2是本实验室使用Neptune型ICP-MS在高分辨模式下的多接收测试结果,在曲线左侧平台上分析可得到样品真正的Fe⁺信号,从而有效地将干扰去除^[33]。

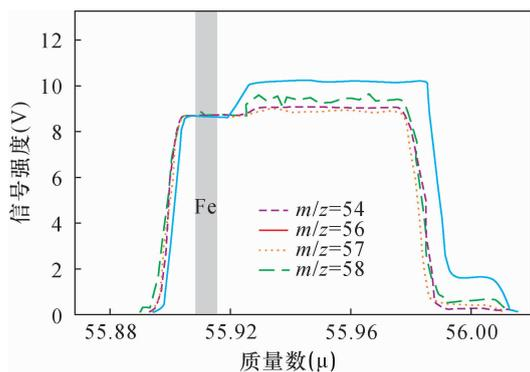


图2 高分辨率模式下铁同位素与干扰峰的谱峰^[33]
(所有谱峰放大到⁵⁶Fe水平)

Fig. 2 Peak shape of Fe isotopes and interfering signals at high-resolution mode^[33]

虽然MC-ICP-MS可以将干扰元素和目标同位素有效分开,但其在同位素分析过程中会产生较大的质量歧视(达3%/amu),必须对仪器的质量歧视进行准确校正^[57]。目前对仪器质量歧视的校正方法主要有三种:①标准-样品-标准交叉法(SSB, Standard-Sample-Bracketing)^[29,57-58]。用仪器对样品前后两个已知同位素组成标准的质量歧视来校正仪器对样品的质量歧视。用该方法进行质量歧视校正的前提是,在测试过程中仪器的质量歧视对于样品和标样是相同的。如果测试过程中因样品和标样化学成分不同而导致仪器质量分馏的变化,将会使运用SSB法进行仪器质量校正后的数据偏离真值,这就是所谓的基体效应^[59];②内标法(Cu-doped SSB)^[41,58-60]。向所有样品和标准中加入一种与被测元素质量数相似的元素(如测定铁同位素是加入Cu),通过测量仪器对该元素同位素的质量歧视因子,来校正仪器对被测元素同位素的质量歧视。但是经过分离后样品中可能残留的少量Cu或Ni会使校正结果存在偏差,另外Cu作为内标

时,Cu和Fe不能放在同一个序列(Cycle)内测试,须使用跳峰模式分两个序列进行测试,这样就延长了测试时间,同时要求两个序列测定过程中的仪器条件完全一致;③双稀释剂法(Double Spike Technique)^[61]。双稀释剂法校正不要求100%的样品回收率,但是该方法使用较少,其主要原因是稀释剂需要高度纯化^[62]。三种校正方法中,SSB法是国内外实验室最常用的校正方法。

MC-ICP-MS同位素测试的分析速度相比TIMS大大提升,测试精度提高了10倍以上,可以达到<0.03‰^[63],足以用来分析各种天然样品的铁同位素组成。因此,MC-ICP-MS已被公认为测定铁同位素组成的最佳方法。

2.2 激光剥蚀原位分析法

经过复杂的地质过程后,矿物或岩石样品的铁同位素往往出现不均一,这些微区范围的变化包含着有关矿物和岩石形成条件、古海洋地质环境、古气候变化历史的重要信息。提取这些重要信息,需要相应的微区同位素分析方法^[64]。自从Gray(1985)^[65]报道了将激光剥蚀系统(Laser Ablation System)与ICP-MS联用技术之后,激光微区原位测试技术取得了迅速发展。该方法是通过激光微束将固体样品表面剥蚀发生汽化,输送至ICP电离后再到达质谱进行分析。LA-ICP-MS可以识别微米尺度上稳定同位素的变化,被广泛应用于Ca、Cr、Cu、Zn、Mo、Fe、Mg等重同位素比值的研究^[66-69]。经过30多年的发展,已有不同类型的激光器和ICP-MS进行了联用研究,激光波长从近红外区发展到深紫外区,激光脉宽也经历了从纳秒到飞秒的进步^[70-72]。目前与ICP-MS联用的主要有Nd-YAG激光剥蚀系统和准分子激光器剥蚀系统^[64,72]以及非标激光剥蚀系统。本文主要对纳秒激光器和飞秒激光器的发展进行评述。

2.2.1 纳秒激光器

T. Hirata和T. Ohno最早将纳秒激光(266nm Nd:YAG, 266nm激光是钕钇榴石晶体受激特征谱线1064nm经过四次倍频得到)与MC-ICP-MS联用进行铁同位素原位分析,其目的是为了检测与生物有关的微小矿化,但结果显示铁同位素比值测量的外部结果精度(重复性)约为1‰,无法识别出天然样品中的同位素变化^[73]。随后Graham等^[74]使用同样的紫外激光器与MC-ICP-MS联用进行原位铁同位素测试,对剥蚀室、测试时间、载气等作了调整, $\delta^{57}\text{Fe}$ 精度达0.2‰,从印度尼西亚Grasberg斑

岩矿床中识别出共生黄铁矿和黄铜矿之间的铁同位素分馏达到4‰。Kosler等^[75]使用213nm纳米激光,其对铁陨石和黄铁矿进行微区原位剥蚀铁同位素测试过程中,发现激光剥蚀出不同粒径的气溶胶之间会导致明显的同位素分馏,高达4‰。Horn等^[76]提出纳秒激光剥蚀出气溶胶之间同位素比值之间的变化是由不规则的、不可再生的烧蚀引起的热诱导效应(熔化、缩合)和粒度效应导致质谱仪产生的质量歧视现象,而不是由不同粒径气溶胶本身造成的。

2.2.2 飞秒激光器

为了克服纳秒激光剥蚀引起的同位素分馏,Horn等^[72]第一次使用了196nm紫外飞秒激光器(脉冲宽度为100~200fs)对铁金属、硫化物、赤铁矿、菱铁矿、针铁矿和磁铁矿进行了测试,均使用IRMM-014作为标样,测试精度达到0.1‰,提出飞秒激光剥蚀电感耦合等离子体质谱法测定铁同位素不需要使用与样品性质匹配的内标。d'Abzac等^[77]发现飞秒激光剥蚀出的不同粒径气溶胶的铁同位素组成有差异,不同的矿物分馏程度也不同,d'Abzac指出这种同位素差异是由冷凝过程中的动力学分馏造成的。为了减少飞秒激光烧蚀过程中的质量分馏,需要确保不同粒径的气溶胶都被有效电离。d'Abzac等^[78]提出通过使用双剥蚀室可以快速提取气溶胶(<0.7s)以减少气溶胶间相互碰撞的几率,能有效减小不同粒径气溶胶之间的这种质量分馏,黄铁矿 $\delta^{56}\text{Fe}$ 精度达0.24‰。

飞秒激光器是在纳秒激光基础上发展起来的短脉冲激光器,脉冲持续时间极短、脉冲峰值强度(功率)极高、聚焦强度(功率密度)超过 $10^{20}\text{W}/\text{cm}^2$,剥蚀过程中能量损耗的机理与纳秒激光不同^[79]。这些特性使得飞秒激光剥蚀电感耦合等离子体质谱具有较高的精度和便捷度,利用飞秒激光电感耦合等离子体质谱测定微区铁同位素研究受到了越来越多的关注^[80-83]。虽然飞秒激光剥蚀在进行铁同位素测试时具有明显的优势,但是和纳秒激光器一样,飞秒激光器在烧蚀、气溶胶迁移以及在电离过程中也会导致铁的同位素分馏^[84],近年来科学家们在对比纳秒激光剥蚀和飞秒激光剥蚀对铁同位素造成的分馏机理方面仍然在不断地探索。

(1)大部分报道认为,纳秒激光脉冲宽度相对比较长,大于电子和晶格声子之间热平衡所需的时间,能量会通过晶格的加热从表面电子传播到内部,形成熔蚀层,从而导致剥蚀坑周围会出现大量熔蚀

物。此外,纳秒激光在剥蚀过程中会在样品上产生微小的裂纹,有可能损坏样品^[85-86]。飞秒激光由于是短脉冲激光, 10^{-15}s 的脉冲宽度比电子晶格加热所需的时间要短,在烧蚀过程中不会出现显著的常规加热,能有效地避免热效应和样品结构的更改^[87-88],并能防止剥蚀点的熔融,消除同位素的分馏效应^[84]。

(2)飞秒激光剥蚀出的颗粒为纳米尺度($1\mu\text{m}$),离子可以被有效地传输和电离(图3)^[89-91]。且无论样品性质和激光条件如何,相比较纳米激光,飞秒激光都能提供基本一致的粒度分布和化学计量取样结果,灵敏度、稳定性和准确度都更高^[77-78,92]。

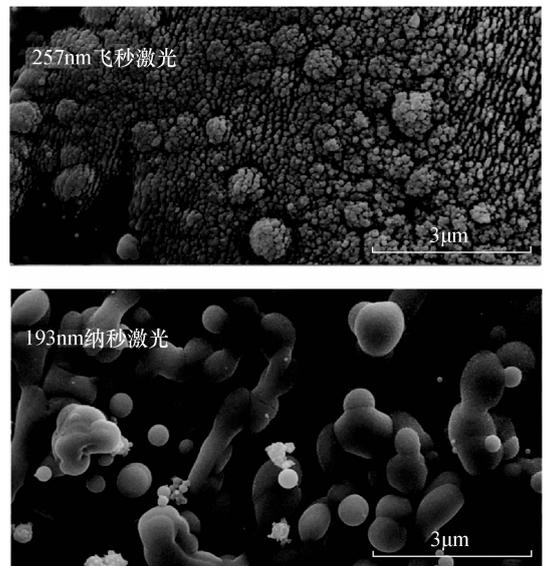


图3 飞秒激光和纳秒激光剥蚀出气溶胶的粒径对比^[91]
Fig. 3 Comparison of aerosols from femtosecond laser ablation and nanosecond laser ablation in ilmenite^[91]

(3)飞秒激光和纳秒激光分析中均会出现基体效应。Zheng等(2018)^[93]的研究表明飞秒激光分析出现的基体效应几乎可以通过在分析过程中引入水蒸汽来完全抑制,测试精度和准确度可以达到0.1‰左右,不需要样品和标准之间的基体匹配。Teng等(2010)^[94]和Janney等(2011)^[95]也提出类似的观点,在通过溶液雾化或激光烧蚀进行元素和同位素分析时,湿等离子体条件通常比干等离子体更能耐受基体效应。但纳秒激光器通过这一方法却不能有效地抑制基体效应(图4)^[93],在同位素分析中必须进行基体匹配^[92]。在进行严格基体匹配和位置效应评估的情况下,纳秒激光器也会得到高精

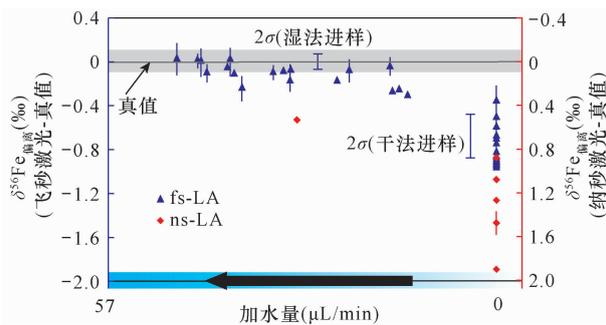


图4 水蒸汽对飞秒激光和纳秒激光基质效应的抑制对比^[93]

Fig. 4 Comparison of nature of matrix effects during *in-situ* Fe isotope analysis between fs-laser and ns-laser ablation^[93]

度测量结果,如 Sio 等^[96]采用波长 193nm 准分子纳米激光器对橄榄石铁同位素进行测定,得到 $\delta^{56}\text{Fe}$ 精度为 0.4‰。

激光原位铁同位素分析能揭示细微区域变化的重要信息,同时也避免了冗长繁琐的化学处理,效率明显提高,但飞秒激光剥蚀系统的购买和维修费用很高,基体效应的存在使得 LA-MC-ICP-MS 的应用仍然受到限制。

3 展望

铁同位素作为非传统稳定同位素体系之一,可为揭示铁的复杂地球化学行为提供独特的依据。随着 MC-ICP-MS 测试技术的不断进步,铁同位素分析精度得到了显著的提高,使得铁同位素在生物学、地球科学、环境学和宇宙科学等领域的应用得到了快速的发展。用于铁同位素测定的溶液法和激光微区原位铁同位素分析,都有其自身的优缺点。溶液法的分析流程长且复杂,但分析精度高、方法稳定。微区原位分析方法的分析速度快、空间分辨率高,为从微观角度探讨地球科学问题提供了可能,纵然活性基体的引入可能会降低甚至消除基体效应的影响,但基体效应的存在限制了它的广泛应用,因而开发系列基体匹配的标样显得尤为重要。

4 参考文献

- [1] Beard B L, Johnson C M. High precision iron isotope measurements of terrestrial and lunar materials [J]. *Geochimica et Cosmochimica Acta*, 1999, 63(11-12): 1653-1660.
- [2] 刘英俊,曹励明,李兆麟. 元素地球化学[M]. 北京: 科学出版社, 1984.

- [3] Liu Y J, Cao L M, Li Z L. *Element Geochemistry* [M]. Beijing: Science Press, 1984.
- [4] 牟保磊. 元素地球化学[M]. 北京: 北京大学出版社, 1999.
- [5] Mu B L. *Element Geochemistry* [M]. Beijing: Peking University Press, 1999.
- [6] Dauphas N, John S G, Rouxel O. Iron isotope systematics [J]. *Reviews in Mineralogy and Geochemistry*, 2017, 82(1): 415-510.
- [7] 何永胜, 胡东平, 朱传卫. 地球科学中铁同位素研究进展[J]. *地学前缘*, 2015, 22(5): 54-71.
- [8] He Y S, Hu D P, Zhu C W. Progress of iron isotope geochemistry in geoscience [J]. *Earth Science Frontiers*, 2015, 22(5): 54-71.
- [9] Beard B L, Johnson C M, Skulan J L, et al. Application of Fe isotopes to tracing the geochemical and biological cycling of Fe [J]. *Chemical Geology*, 2003, 195(1): 87-117.
- [10] Johnson C M, Beard B L, Roden E E. The iron isotope fingerprints of redox and biogeochemical cycling in modern and ancient earth [J]. *Annual Review of Earth and Planetary Sciences*, 2008, 36(1): 457-493.
- [11] Dauphas N, Rouxel O. Mass spectrometry and natural variations of iron isotopes [J]. *Mass Spectrometry Reviews*, 2006, 25: 515-550.
- [12] Beard B L, Johnson C M, von Damm K L, et al. Iron isotope constraints on Fe cycling and mass balance in oxygenated Earth oceans [J]. *Geology*, 2003, 31(7): 629-632.
- [13] Kodolányi J, Stephan T, Trappitsch R, et al. Iron and nickel isotope compositions of presolar silicon carbide grains from supernovae [J]. *Geochimica et Cosmochimica Acta*, 2018, 221: 127-144.
- [14] Conway T M, John S G. Quantification of dissolved iron sources to the North Atlantic Ocean [J]. *Nature*, 2014, 511(7508): 212-215.
- [15] Anbar A D. Iron stable isotopes: Beyond biosignatures [J]. *Earth and Planetary Science Letters*, 2004, 217(3): 223-236.
- [16] Labidi J. Iron Isotope Composition of Depleted MORB [C]//Proceedings of Agu Fall Meeting (AGU Fall Meeting Abstracts), 2015.
- [17] Teng F Z, Dauphas N, Huang S, et al. Iron isotopic systematics of oceanic basalts [J]. *Geochimica et Cosmochimica Acta*, 2013, 107: 12-26.
- [18] Sossi P A, Nebel O, Anand M, et al. On the iron isotope composition of Mars and volatile depletion in the terrestrial planets [J]. *Earth and Planetary Science Letters*, 2016, 449: 360-371.
- [19] Sossi P A, O'Neill H St C. The effect of bonding

- environment on iron isotope fractionation between minerals at high temperature [J]. *Geochimica et Cosmochimica Acta*, 2016, 196: 121 – 143.
- [17] Rouxel O, Toner B M, Manganini S J, et al. Geochemistry and iron isotope systematics of hydrothermal plume fall – out at East Pacific Rise 9°50'N [J]. *Chemical Geology*, 2016, 441: 212 – 234.
- [18] Weyer S, Ionov D A. Partial melting and melt percolation in the mantle: The message from Fe isotopes [J]. *Earth and Planetary Science Letters*, 2007, 259: 119 – 133.
- [19] Zhao Y, Xue C J, Liu S A, et al. Redox reactions control Cu and Fe isotope fractionation in a magmatic Ni – Cu mineralization system [J]. *Geochimica et Cosmochimica Acta*, 2019, 249(15): 42 – 58.
- [20] Syverson D D, Luhmann A J, Tan C, et al. Fe isotope fractionation between chalcopyrite and dissolved Fe during hydrothermal recrystallization: An experimental study at 350°C and 500bars [J]. *Geochimica et Cosmochimica Acta*, 2017, 200: 87 – 109.
- [21] Williams K B, Krawczynski M J, Nie N X, et al. The Role of Differentiation Processes in Mare Basalt Iron Isotope Signatures [C]//Proceedings of Lunar and Planetary Science Conference, 2016.
- [22] Bau M, von Blanckenburg F, Ohmoto H. Iron isotope stratification of Late Archean Seawater: Evidence from dolomites and banded iron – formations [J]. *Nature Immunology*, 2017, 16(5): 467 – 75.
- [23] McCoy V E, Asael D, Planavsky N. Benthic iron cycling in a high – oxygen environment: Implications for interpreting the Archean sedimentary iron isotope record [J]. *Geobiology*, 2017, 15(5): 619 – 627.
- [24] Liu K, Wu L L, Couture R M, et al. Iron isotope fractionation in sediments of an oligotrophic freshwater lake [J]. *Earth and Planetary Science Letters*, 2015, 423: 164 – 172.
- [25] Kurzweil F, Pasava J, Drost K, et al. Molybdenum (Mo) and Iron (Fe) Isotope Evidence of Tepla – Barrandian Black Shales against Widespread Deep Ocean Oxygenation in the Late Neoproterozoic [C]//Proceedings of the Fall Meeting 2014. American Geophysical Union, 2014.
- [26] Severmann S, Lyons T W, Anbar A, et al. Modern iron isotope perspective on the benthic iron shuttle and the redox evolution of ancient oceans [J]. *Geology*, 2008, 36(6): 487 – 490.
- [27] Shollenberger Q R, Brennecke G A, Schuth S, et al. Iron Isotope Systematics of Refractory Inclusions and the Search for the Source of Nucleosynthetic Anomalies [C]//Proceedings of the 48th Lunar and Planetary Science Conference, 2017.
- [28] Poitrasson F, Halliday A N, Lee D C, et al. Iron isotope differences between Earth, Moon, Mars and Vesta as possible records of contrasted accretion mechanisms [J]. *Earth and Planetary Science Letters*, 2004, 223(3 – 4): 0 – 266.
- [29] Belshaw N S, Zhu X K, Guo Y, et al. High precision measurement of iron isotopes by plasma source mass spectrometry [J]. *International Journal of Mass Spectrometry*, 2000, 197(1 – 3): 191 – 195.
- [30] 唐索寒, 朱祥坤, 李津, 等. 用于多接收器等离子体质谱测定的铁铜锌同位素标准溶液研制 [J]. *岩矿测试*, 2016, 35(2): 127 – 133.
- Tang S H, Zhu X K, Li J, et al. New standard solutions for measurement of iron, copper and zinc isotopic compositions by multi – collector inductively coupled plasma – mass spectrometry [J]. *Rock and Mineral Analysis*, 2016, 35(2): 127 – 133.
- [31] 孙剑, 朱祥坤, 陈岳龙. 碳酸盐矿物铁同位素测试的选择性溶解方法研究——以白云鄂博矿床赋矿白云岩为例 [J]. *岩矿测试*, 2013, 32(1): 28 – 33.
- Sun J, Zhu X K, Chen Y L. The selective dissolution of carbonate minerals for Fe isotope determination: A case study on the ore – hosting dolomite marble in the Bayan Obo ore deposit [J]. *Rock and Mineral Analysis*, 2013, 32(1): 28 – 33.
- [32] 唐索寒, 闫斌, 朱祥坤, 等. 玄武岩标准样品铁铜锌同位素组成 [J]. *岩矿测试*, 2012, 31(2): 218 – 224.
- Tang S H, Yan B, Zhu X K, et al. Iron, copper and zinc isotopic compositions of basaltic standard reference materials [J]. *Rock and Mineral Analysis*, 2012, 31(2): 218 – 224.
- [33] 侯可军, 秦燕, 李延河. Fe 同位素的 MC – ICP – MS 测试方法 [J]. *地球学报*, 2012, 33(6): 885 – 892.
- Hou K J, Qin Y, Li Y H. High – precision measurements of Fe isotopes using MC – ICP – MS [J]. *Acta Geoscientica Sinica*, 2012, 33(6): 885 – 892.
- [34] Zhu X K, Guo Y, Williams R J P, et al. Mass fractionation processes of transition metal isotopes [J]. *Earth and Planetary Science Letters*, 2002, 200(1 – 2): 47 – 62.
- [35] Rosman K J R, Taylor P D P. Isotopic compositions of the elements 1997 (Technical Report) [J]. *Pure and Applied Chemistry*, 1998, 70(1): 217 – 235.
- [36] Kraus K A, Moore G E. Anion exchange studies: The divalent transition elements manganese to zinc in hydrochloric acid [J]. *Journal of the American Chemical Society*, 1953, 75: 1460 – 1462.
- [37] Kosler J, Pedersen R B, Kruber C, et al. Comment on “Analysis of Fe isotopes in sulfides and iron meteorites by laser ablation high – mass resolution multi – collector – ICP mass spectrometry” —Reply [J]. *Journal of Analytical*

- Atomic Spectrometry, 2006, 21(2): 214 – 216.
- [38] Strelow F W E. Improved separation of iron from copper and other elements by anion – exchange chromatography on a 4% cross – linked resin with high concentrations of hydrochloric acid [J]. *Talanta*, 1980, 27(9): 727 – 732.
- [39] Anbar A D. Nonbiological fractionation of iron isotopes [J]. *Science*, 2000, 288(5463): 126 – 128.
- [40] Dauphas N, Janney P E, Mendybaev R A, et al. Chromatographic separation and multicollection ICPMS analysis of iron. Investigating mass – dependent and independent isotope effects [J]. *Analytical Chemistry*, 2004, 76(19): 5855 – 5863.
- [41] van der Walt T N, Strelow F W E, Haasbroek F J. Separation of iron – 52 from chromium cyclotron targets on the 2% cross – linked anion – exchange resin AG1 – X2 in hydrochloric acid [J]. *Talanta*, 1985, 32(4): 313 – 317.
- [42] Marechal C N. Precise analysis of copper and zinc isotopic compositions by plasma – source mass spectrometry [J]. *Chemical Geology*, 1999, 156(1 – 4): 251 – 273.
- [43] Archer C, Vance D. Mass discrimination correction in multiple – collector plasma source mass spectrometry: An example using Cu and Zn isotopes [J]. *Journal of Analytical Atomic Spectrometry*, 2004, 19(5): 656 – 665.
- [44] Sossi P A, Halverson G P, Nebel O, et al. Combined separation of Cu, Fe and Zn from rock matrices and improved analytical protocols for stable isotope determination [J]. *Geostandards and Geoanalytical Research*, 2015, 39(2): 129 – 149.
- [45] Poitrasson F, Freyrier R. Heavy iron isotope composition of granites determined by high resolution MC – ICP – MS [J]. *Chemical Geology*, 2005, 222(1): 132 – 147.
- [46] 唐索寒, 闫斌, 李津. 少量 AG1 – X4 阴离子交换树脂分离地质标样中的铁及铁同位素测定 [J]. *地球化学*, 2013(1): 46 – 52.
Tang S H, Yan B, Li J. Separation of Fe using a small amount of AG1 – X4 anion exchange resin and Fe isotope compositions of geological reference materials [J]. *Geochimica*, 2013(1): 46 – 52.
- [47] 马信江, 梁细荣, 涂相林, 等. AG MP – 1M 阴离子分离 Cu, Fe, Zn 及其在 Fe 同位素测定上的应用 [J]. *地球化学*, 2009, 38(5): 70 – 76.
Ma X J, Liang X R, Tu X L, et al. Separation of Cu, Fe and Zn using AG MP – 1M anion exchange resin and applications for Fe isotope determination [J]. *Geochimica*, 2009, 38(5): 70 – 76.
- [48] 孙剑, 朱祥坤, 唐索寒, 等. AG MP – 1 阴离子交换树脂元素分离方法再研究 [J]. *高校地质学报*, 2006, 24(3): 398 – 403.
Sun J, Zhu X K, Tang S H, et al. Further investigation on elemental separation using AG MP – 1 anion exchange resin [J]. *Geological Journal of China Universities*, 2006, 24(3): 398 – 403.
- [49] Craddock P R, Dauphas N. Iron isotopic compositions of geological reference materials and chondrites [J]. *Geostandards and Geoanalytical Research*, 2011, 35(1): 101 – 123.
- [50] Sossi P A, Halverson G P, Nebel O, et al. Combined separation of Cu, Fe and Zn from rock matrices and improved analytical protocols for stable isotope determination [J]. *Geostandards and Geoanalytical Research*, 2015, 39(2): 129 – 149.
- [51] Liu S A, Li D, Li S, et al. High – precision copper and iron isotope analysis of igneous rock standards by MC – ICP – MS [J]. *Journal of Analytical Atomic Spectrometry*, 2013, 29(1): 122 – 133.
- [52] Taylor P D P, Maecck R, Bièvre P D. Determination of the absolute isotopic composition and atomic weight of a reference sample of natural iron [J]. *International Journal of Mass Spectrometry and Ion Processes*, 1992, 121(1 – 2): 111 – 125.
- [53] Rudge J F, Reynolds B C, Bourdon B. The double spike toolbox [J]. *Chemical Geology*, 2009, 265(3 – 4): 0 – 431.
- [54] Zhu X K, Makishima A, Guo Y, et al. High precision measurement of titanium isotope ratios by plasma source mass spectrometry [J]. *International Journal of Mass Spectrometry*, 2002, 220(1): 21 – 29.
- [55] Kehm K, Hauri E H, Alexander C M O, et al. High precision iron isotope measurements of meteoritic material by cold plasma ICP – MS [J]. *Geochimica et Cosmochimica Acta*, 2003, 67(15): 2879 – 2891.
- [56] Weyer S, Schwieters J. High precision Fe isotope measurements with high mass resolution MC – ICPMS [J]. *International Journal of Mass Spectrometry*, 2003, 226: 355 – 368.
- [57] 朱祥坤, 李志红, 赵新苗, 等. 铁同位素的 MC – ICP – MS 测定方法与地质标准物质的铁同位素组成 [J]. *岩石矿物学杂志*, 2008, 27(4): 263 – 272.
Zhu X K, Li Z H, Zhao X M, et al. High – precision measurement of Fe isotopes isotopes using MC – ICP – MS and Fe isotope compositions of geological reference materials [J]. *Acta Petrologica et Mineralogica*, 2008, 27(4): 263 – 272.
- [58] 唐索寒, 朱祥坤, 蔡俊军, 等. 用于多接收器等离子体质谱铜铁锌同位素测定的离子交换分离方法 [J]. *岩矿测试*, 2006, 25(1): 5 – 8.
Tang S H, Zhu X K, Cai J J, et al. Chromatographic separation of Cu, Fe and Zn using AG MP – 1 anion

- exchange resin for isotope determination by MC – ICPMS [J]. *Rock and Mineral Analysis*, 2006, 25(1): 5 – 8.
- [59] Zhu X K, O' Nions R K, Guo Y, et al. Determination of natural Cu – isotope variation by plasma – source mass spectrometry: Implications for use as geochemical tracers [J]. *Chemical Geology*, 2000, 163(1): 139 – 149.
- [60] Arnold T, Markovic T, Kirk G J D, et al. Iron and zinc isotope fractionation during uptake and translocation in rice (*Oryza sativa*) grown in oxic and anoxic soils [J]. *Comptes Rendus Geoscience*, 2015, 347 (7 – 8): 397 – 404.
- [61] Dideriksen K, Baker J A, Stipp S L S. Iron isotopes in natural carbonate minerals determined by MC – ICP – MS with a $^{58}\text{Fe} - ^{54}\text{Fe}$ double spike [J]. *Geochimica et Cosmochimica Acta*, 2006, 70(1): 0 – 132.
- [62] Rudge J F, Reynolds B C, Bourdon B. The double – spike toolbox [J]. *Chemical Geology*, 2009, 265(3 – 4): 420 – 431.
- [63] Dauphas N, Pourmand A, Teng F Z. Routine isotopic analysis of iron by HR – MC – ICPMS: How precise and how accurate? [J]. *Chemical Geology*, 2009, 267(3 – 4): 0 – 184.
- [64] 丁梯平. 激光探针稳定同位素分析技术的现状及发展前景 [J]. *地学前缘*, 2003, 10(2): 263 – 268.
Ding T P. The present status and prospect on laser – microprobe analysis techniques for stable isotopes [J]. *Earth Science Frontiers*, 2003, 10(2): 263 – 268.
- [65] Gray A L. Solid sample introduction by laser ablation for inductively coupled plasma source mass spectrometry [J]. *Analyst*, 1985, 110: 551.
- [66] Horn I, Hinton R W, Jackson S E, et al. Ultra – trace element analysis of NIST SRM 616 and 614 using laser ablation microprobe – inductively coupled plasma – mass spectrometry (LAM – ICP – MS): A comparison with secondary ion mass spectrometry (SIMS) [J]. *Geostandards and Geoanalytical Research*, 2010, 21(2): 191 – 203.
- [67] Horn I, Rudnick R L, McDonough W F. Precise elemental and isotope ratio determination by simultaneous solution nebulization and laser ablation – ICP – MS: Application to U – Pb geochronology [J]. *Chemical Geology*, 2000, 164(3): 281 – 301.
- [68] Mank A J G, Mason P R D. A critical assessment of laser ablation ICP – MS as an analytical tool for depth analysis in silica – based glass samples [J]. *Journal of Analytical Atomic Spectrometry*, 1999, 14(8): 1143 – 1153.
- [69] Günther D, Heinrich C A. Enhanced sensitivity in laser ablation – ICP mass spectrometry using helium – argon mixtures as aerosol carrier [J]. *Journal of Analytical Atomic Spectrometry*, 1999, 14 (9): 1363 – 1368.
- [70] Arrowsmith P. Laser ablation of solids for elemental analysis by inductively coupled plasma mass spectrometry [J]. *Analytical Chemistry*, 1987, 59: 10 (10): 1437 – 1444.
- [71] Norman M D, Pearson N J, Sharma A, et al. Quantitative analysis of trace elements in geological materials by laser ablation ICPMS: Instrumental operating conditions and calibration values of NIST glasses [J]. *Geostandards and Geoanalytical Research*, 2010, 20(2): 247 – 261.
- [72] Horn I, von Blanckenburg F, Schoenberg R, et al. *In situ* iron isotope ratio determination using UV – femtosecond laser ablation with application to hydrothermal ore formation processes [J]. *Geochimica et Cosmochimica Acta*, 2006, 70: 3677 – 3688.
- [73] Hirata T, Ohno T. *In – situ* isotopic ratio analysis of iron using laser ablation – multiple collector – inductively coupled plasma mass spectrometry (LA – MC – ICP – MS) [J]. *Journal of Analytical Atomic Spectrometry*, 2001, 16(5): 487 – 491.
- [74] Graham S, Pearson N, Jackson S, et al. Tracing Cu and Fe from source to porphyry: *In situ* determination of Cu and Fe isotope ratios in sulfides from the Grasberg Cu – Au deposit [J]. *Chemical Geology*, 2004, 207 (3): 147 – 169.
- [75] Kosler J, Pedersen R B, Kruber C, et al. Analysis of Fe isotopes in sulfides and iron meteorites by laser ablation high – mass resolution multi – collector ICP mass spectrometry [J]. *Journal of Analytical Atomic Spectrometry*, 2005, 21: 192 – 199.
- [76] Horn I, Schoenberg R, Blanckenburg F V. Comment on “Analysis of Fe isotopes in sulfides and iron meteorites by laser ablation high – mass resolution multi – collector – ICP mass spectrometry” by J. Košler, R. B. Pedersen, C. Kruber and P. J. Sylvester [J]. *Journal of Analytical Atomic Spectrometry*, 2006, 21(2): 211 – 213.
- [77] d' Abzac F X, Beard B L, Czaja A D, et al. Iron isotope composition of particles produced by UV – femtosecond laser ablation of natural oxides, sulfides, and carbonates [J]. *Analytical Chemistry*, 2013, 85 (24): 11885 – 11892.
- [78] d' Abzac F X, Czaja A D, Beard B L, et al. Iron distribution in size – resolved aerosols generated by UV – femtosecond laser ablation: Influence of cell geometry and implications for *in situ* isotopic determination by LA – MC – ICP – MS [J]. *Geostandards and Geoanalytical Research*, 2014, 38 (3): 293 – 309.
- [79] Oeser M, Weyer S, Horn I, et al. High – precision Fe and Mg isotope ratios of silicate reference glasses determined *in situ* by femtosecond LA – MC – ICP – MS and by

- solution nebulisation MC – ICP – MS [J]. Geostandards and Geoanalytical Research, 2014, 38: 311 – 328.
- [80] Oeser M, Dohmen R, Horn I, et al. Processes and time scales of magmatic evolution as revealed by Fe – Mg chemical and isotopic zoning in natural olivines [J]. Geochimica et Cosmochimica Acta, 2015, 154: 130 – 150.
- [81] Teng F Z, Dauphas N, Helz R T, et al. Diffusion – driven magnesium and iron isotope fractionation in Hawaiian olivine [J]. Earth and Planetary Science Letters, 2011, 308(3 – 4): 0 – 324.
- [82] Corliss K I S, Dauphas N. Thermal and crystallization histories of magmatic bodies by Monte Carlo inversion of Mg – Fe isotopic profiles in olivine [J]. Geology, 2017, 45(1): 67 – 70.
- [83] Collinet M, Charlier B, Namur O, et al. Crystallization history of enriched shergottites from Fe and Mg isotope fractionation in olivine megacrysts [J]. Geochimica et Cosmochimica Acta, 2017, 207: 277 – 297.
- [84] Horn I, von Blanckenburg F. Investigation on elemental and isotopic fractionation during 196nm femtosecond laser ablation multiple collector inductively coupled plasma mass spectrometry [J]. Spectrochim Acta Part B: Atomic Spectroscopy, 2007, 62: 410 – 422.
- [85] Öder H R. Laser – generated aerosols in laser ablation for inductively coupled plasma spectrometry [J]. Spectrochimica Acta Part B: Atomic Spectroscopy, 2006, 61(3): 284 – 300.
- [86] Momma C, Chichkov B N, Nolte S, et al. Short – pulse laser ablation of solid targets [J]. Optics Communications, 1996, 129(1 – 2): 134 – 142.
- [87] Russo R E, Mao X, Gonzalez J J, et al. Femtosecond vs. nanosecond laser pulse duration for laser ablation chemical analysis [J]. Spectroscopy, 2013, 28(1): 24 – 39.
- [88] Günther D, Hattendorf B. Solid sample analysis using laser ablation inductively coupled plasma mass spectrometry [J]. TrAC Trends in Analytical Chemistry, 2005, 24(3): 255 – 265.
- [89] Koch J, von Bohlen A, Hergenröder R, et al. Particle size distributions and compositions of aerosols produced by near – IR femto – and nanosecond laser ablation of brass [J]. Journal of Analytical Atomic Spectrometry, 2004, 19(2): 267 – 272.
- [90] 陈开运, 范超, 袁洪林, 等. 飞秒激光剥蚀 – 多接收电感耦合等离子体质谱原位微区分析青铜中铅同位素组成——以古铜钱币为例 [J]. 光谱学与光谱分析, 2013, 32(5): 1342 – 1349.
- Chen K Y, Fan C, Yuan H L, et al. High – precision *in situ* analysis of the lead isotopic composition in copper using femtosecond laser ablation MC – ICP – MS and the application in ancient coins [J]. Spectroscopy and Spectral Analysis, 2013, 32(5): 1342 – 1349.
- [91] 杨文武, 史光宇, 商琦, 等. 飞秒激光剥蚀电感耦合等离子体质谱在地球科学中的应用进展 [J]. 光谱学与光谱分析, 2017, 37(7): 208 – 214.
- Yang W W, Shi G Y, Shang Q, et al. Applications of femtosecond (fs) laser ablation – inductively coupled plasma – mass spectrometry in Earth sciences [J]. Spectroscopy and Spectral Analysis, 2017, 37(7): 208 – 214.
- [92] Zheng X Y, Beard B L, Lee S, et al. Contrasting particle size distributions and Fe isotope fractionations during nanosecond and femtosecond laser ablation of Fe minerals: Implications for LA – MC – ICP – MS analysis of stable isotopes [J]. Chemical Geology, 2017, 450: 235 – 247.
- [93] Zheng X Y, Beard B L, Johnson C M. Assessment of matrix effects associated with Fe isotope analysis using 266nm femtosecond and 193nm nanosecond laser ablation multi – collector inductively coupled plasma mass spectrometry [J]. Journal of Analytical Atomic Spectrometry, 2018, 33: 68 – 83.
- [94] Teng F Z, Li W Y, Ke S, et al. Magnesium isotopic composition of the Earth and chondrites [J]. Geochimica et Cosmochimica Acta, 2010, 74(14): 4150 – 4166.
- [95] Janney P E, Richter F M, Mendybaev R A, et al. Matrix effects in the analysis of Mg and Si isotope ratios in natural and synthetic glasses by laser ablation – multicollector ICPMS: A comparison of single – and double – focusing mass spectrometers [J]. Chemical Geology, 2011, 281(1 – 2): 26 – 40.
- [96] Sio C K I, Dauphas N, Teng F Z, et al. Discerning crystal growth from diffusion profiles in zoned olivine by *in situ* Mg – Fe isotopic analyses [J]. Geochimica et Cosmochimica Acta, 2013, 123(2): 302 – 321.

Progress of Analytical Techniques for Stable Iron Isotopes

QIN Yan¹, XU Yan - ming², HOU Ke - jun^{1*}, LI Yan - he¹, CHEN Lei¹

(1. Key Laboratory of Metallogeny and Mineral Assessment, Ministry of National Resources; Institute of Mineral Resources, Chinese Academy of Geological Sciences, Beijing 100037, China;

2. Qingdao Geological Engineering Survey Institute (Qingdao Geological Exploration and Development Bureau), Qingdao 266071, China)

HIGHLIGHTS

(1) Recent advances in Fe isotope analyses were reviewed.

(2) The mechanism and correction method of isotopic fractionation during mass spectrometry analysis were summarized.

(3) The advantages and disadvantages of solution and *in situ* methods for Fe isotope analyses were compared.

ABSTRACT

BACKGROUND: Iron is the most abundant element on earth with variable valences. It is widely distributed in various minerals, rocks, fluids and organisms, and is involved in diagenesis, mineralization, hydrothermal activities and life activities. The study of iron isotope composition provides important information for geochemistry, astrochemistry and biochemistry. The accurate measurement of Fe isotopes is an important basis for the development of related research.

OBJECTIVES: To summarize the research progress of Fe isotope measurement technology.

METHODS: The current chemical separation and purification methods and main instrumental analysis techniques commonly used for iron isotopes, were compared and analyzed in this review, and the mechanism of different types of fractionations during mass spectrometry were discussed. These advances included: (1) Improvement of anion resin during determination of iron isotope by solution method; (2) Mass spectrometry development from traditional thermal ionization mass spectrometry to multi - collector inductively coupled plasma mass spectrometry; (3) Development of laser *in situ* analytical technology. On this basis, the steps and calibration methods that would cause iron isotope fractionation during the analysis were summarized, and the advantages and disadvantages of different analytical methods were reviewed.

RESULTS: The analysis process of solution method was long and complicated, but the precision was high (0.03‰, 2SD) and the method was stable. *In situ* iron isotope analysis method developed from nanosecond laser denudation to femtosecond laser denudation, with shorter pulse duration, higher pulse peak intensity (up to 10¹²W), and focusing intensity exceeding 10²⁰W/cm². *In situ* iron isotope analysis method was fast and had high spatial resolution, which can be used to discuss the geochemical process from the microscopic perspective. However, the presence of matrix effects limited the widespread use of iron isotopes.

CONCLUSIONS: Shortening solution analysis process and developing a series of matrix - matched standard samples are the research direction of iron isotope analysis.

KEY WORDS: iron isotope; chemical separation; solution method; mass spectrometry; laser ablation; matrix effect